## Nuclear Shadowing and High- $p_T$ Hadron Spectra in Relativistic Heavy Ion Collisions

S. R. Klein $^1$  and R. Vogt $^{1,2}$ 

<sup>1</sup>Nuclear Science Division, Lawrence Berkeley National Laboratory, Berkeley, CA 94720, USA

<sup>2</sup>Physics Department, University of California, Davis, CA 95616, USA

## Abstract

We explore how nuclear modifications to the nucleon parton distributions affect production of high- $p_T$  hadrons in heavy ion collisions. We perform a leading order calculation of the high- $p_T$  charged pion, kaon and proton spectra using standard fragmentation functions and shadowing parameterizations. We also consider alternate models of shadowing. Near midrapidity, shadowing is a small effect and cannot explain the large observed suppression of high- $p_T$  hadrons. We also consider the isospin difference between protons and nuclei and find that it is also a small effect on high- $p_T$  hadron production.

Some of the most interesting experimental results to come out of the Relativistic Heavy Ion Collider (RHIC) at Brookhaven National Laboratory have involved the observed suppression of high- $p_T$  hadron production in collisions of gold nuclei at a center of mass energy,  $\sqrt{S_{NN}}$ , of 130 and 200 GeV per nucleon. Both the PHENIX [1] and STAR [2] collaborations have published results showing that production of hadrons with transverse momentum  $p_T > 2 \text{ GeV}/c$  are suppressed compared to the pp reference spectrum convoluted with the number of binary collisions. The suppression is given in terms of the ratio

$$R_{AA}(p_T) = \frac{d\sigma_{AA}/dp_T}{T_{AA}d\sigma_{m}/dp_T} \tag{1}$$

where  $d\sigma_{AA}/dp_T$  and  $d\sigma_{pp}/dp_T$  are the hadron  $p_T$  distributions in AA and pp collisions respectively and  $T_{AA}$  is the nuclear overlap function. The product of the inelastic nucleon-nucleon cross section with the nuclear overlap function is the number of binary nucleon-nucleon collisions in a given impact parameter range.

The data show that, for  $p_T > 2$  GeV/c,  $R_{AA}(p_T)$  is much less than 1. For charged hadrons (pions, protons and kaons),  $R_{AA}(p_T) \approx 0.4$  [1,2], while for  $\pi^0$ ,  $R_{AA}(p_T) \approx 0.3$  [1]. It appears that, for protons, there is very little suppression, with  $R_{AA}(p_T) \approx 1.0$  [3]. A related ratio has been formed for central to peripheral collisions which produce low multiplicities, such as those in pp interactions. Similar values were found [1,2]. The results at  $\sqrt{S_{NN}} = 130$  GeV and 200 GeV are in agreement with each other.

One possible explanation for the strong suppression is parton energy loss in the medium produced in the collision [4,5]. However, other, more conventional nuclear effects must also be considered. Gold nuclei have a different isospin from the proton reference. Isospin is much less relevant for comparison of central and peripheral ion collisions. More importantly, the parton distributions in nuclei are known to be different from those in bare nucleons [6]. In their analysis, the experimenters noted that this difference, referred to as nuclear shadowing, might affect  $R_{AA}$  but estimated that the change would be small. Here, we give quantitative estimates of the effects of nuclear shadowing and isospin on  $R_{AA}$  for charged pions, kaons and protons separately. The Cronin effect, which broadens the  $p_T$  distributions in pA relative

to pp collisions, tends to increase  $R_{AA}$  [4]. To better illustrate the effects of shadowing and isospin alone, we do not include the Cronin effect in our calculations.

We make a leading order (LO) calculation of minijet production to calculate the yield of high- $p_T$  partons [7]. The  $p_T$  distribution is [8]

$$\frac{d\sigma_{AB}^h}{dp_T} = 2p_T \int_0^{\pi} \frac{d\theta_{\rm cm}}{\sin\theta_{\rm cm}} \int dx_i \int dx_j f_{i/A}(x_i, Q^2) f_{j/B}(x_j, Q^2) \frac{D_{h/k}(z_c)}{z_c} \frac{d\hat{\sigma}}{d\hat{t}}$$
(2)

where x is the fraction of the hadron momentum carried by the interacting parton and Q is the momentum scale of the interaction. The integral over center-of-mass scattering angle  $0 \le \theta_{\rm cm} \le \pi$  corresponds to an integral over all rapidities. The  $2 \to 2$  minijet cross sections are given by  $d\hat{\sigma}/d\hat{t}$ . The fragmentation functions,  $D_{h/k}(z_c)$ , are the probability for the production of hadron h from parton k [9]. The parton densities,  $f_{i/A}(x_i, Q^2)$ , in a nucleus are  $f_{i/A}(x_i) = R_A^i(x_i)(Z_A f_{i/p}(x_i) + N_A f_{i/n}(x_i))/A$  where  $Z_A$  and  $N_A$  are the proton and neutron numbers in nucleus A. We use the MRST LO proton parton distribution functions for isolated nucleons [10] and the EKS98 parameterization of the shadowing function  $R_A^i$  [11]. We take  $Q^2 = p_T^2$ .

In our calculations, we neglect higher-order corrections, using LO parton densities, fragmentation functions, and shadowing parameterizations. Since  $R_{AA}$  is a ratio, the higher-order corrections should largely cancel out. The produced quarks, antiquarks and gluons are fragmented into charged pions, kaons and protons using LO fragmentation functions fit to  $e^+e^-$  data [9]. The final-state hadrons are assumed to be produced pairwise so that  $\pi \equiv (\pi^+ + \pi^-)/2$ ,  $K \equiv (K^+ + K^-)/2$ , and  $p \equiv (p + \overline{p})/2$ . Any baryon asymmetry in the initial state then has no effect on the baryon composition of the final state. The produced hadrons follow the parent parton directions. The  $Q^2$  evolution is modeled using  $e^+e^-$  data at several different energies. These fragmentation functions were also compared to  $p\overline{p}$ ,  $\gamma p$  and  $\gamma \gamma$  data. After some slight scale modifications [12] they were able to fit all the  $h^-$  data. However, there are significant uncertainties in fragmentation when the leading hadron takes most of the parton momentum [13].

Shadowing is assumed to depend only on the parton momentum fraction x, the momen-

tum scale  $Q^2$ , the parton flavor and the nuclear mass number A. The EKS98 parameterization evolves each parton type separately for  $2.25 \le Q^2 \le 10^4 \text{ GeV}^2$ . In the momentum range relevant to RHIC,  $R_A^i$  for quarks and antiquarks are based on nuclear deep-inelastic scattering data. There is very little direct data on the nuclear gluon distribution so that gluon shadowing is primarily based on the  $Q^2$  evolution of the nuclear structure functions. The gluon density shows significant antishadowing for 0.1 < x < 0.3 while the antiquark densities are shadowed in this region. For 0.3 < x < 0.7, there is significant suppression for all partons, the EMC effect, while for x < 0.07, there is also significant suppression.

We do not include inhomogeneous (spatially varying) modifications [14]. Shadowing should be largest near the core of the nucleus and reduced near the surface. In very peripheral collisions, shadowing effects should be sufficiently reduced for pp collisions to be a reasonable model of the most peripheral events. For the most central collisions, the deviation from  $R_{AA} = 1$  differs by less than 1% from than that calculated with homogeneous shadowing.

Minijets come from quarks, antiquarks and gluons produced in the hard scattering. The fragmentation function determines how these partons become final-state hadrons. Figure 1 shows the percentage of charged pions, kaons and protons produced by quarks, antiquarks and gluons as a function of  $p_T$  at central rapidities,  $|y| \leq 1$ , for pp interactions at  $\sqrt{S} = 200$  GeV. Pion production is dominated by gluons up to  $p_T \sim 10$  GeV/c. At higher  $p_T$ , most of the pions come from quarks. For kaons and protons, the crossover between gluon and quark dominance occurs at lower  $p_T$ ,  $p_T \sim 3.5$  GeV/c for kaons and  $\sim 5$  GeV/c for protons. At large  $p_T$ ,  $\sim 75\%$  of kaons and protons are produced by quarks. At larger rapidities and low  $p_T$ , the relative quark and antiquark contributions increase for kaons and protons. In fact, the gluon contribution to kaon production becomes smaller than the quark and antiquark contributions.

Figures 2 and 3 compare the calculated  $R_{AA}$  integrated over all rapidities to that restricted to  $|y| \leq 1$ . The region  $|y| \leq 1$  roughly matches the experimental acceptances. The results shown in Figs. 2 and 3 probe different x regions, as described below. Without fragmentation,  $x_{i,j} = (p_T/\sqrt{S_{NN}})(e^{\pm y_1} + e^{\pm y_2})$  where  $y_1$  and  $y_2$  are the parton rapidities. When

 $y_1 = y_2 = 0$ ,  $x_i = x_j = 2p_T/\sqrt{S_{NN}}$ . For illustration, we assume that the leading hadron of the minijet carries half the parent parton momentum, increasing  $x_i$  by a factor of two. Then the region  $2 \le p_T \le 10$  GeV corresponds to  $0.04 \le x_i \le 0.2$ . In this x range, the EKS98 parameterization has valence quark and gluon antishadowing and sea quark shadowing. The shadowing modifications decrease with  $Q^2$ . Thus the strongest effects are at low  $p_T$  but the overall effect is small. Away from y = 0,  $x_i$  and  $x_j$  are different. One x will decrease into the low x shadowing region while the other will increase into the EMC region. There are stronger modifications in both these regions so that shadowing has a bigger effect in the broader rapidity region. This is most clearly seen for low  $p_T$  in Fig. 2 where shadowing reduces  $R_{AA} \approx 30\%$  for all species. At higher  $p_T$  the effects are smaller and only the proton curve comes close to the data. The large suppression observed at RHIC for mesons is not seen here.

Figure 3 shows that for  $|y| \leq 1$ , shadowing is only a few percent effect due to the restricted x regions. The composition changes, with charged kaons slightly enhanced and protons slightly suppressed compared to charged pions. This difference is due to isospin. The fragmentation functions assume u and s quarks and antiquarks fragment identically to charged kaons [9] so that at large  $p_T$ , charged kaon production is favored in AA collisions relative to pp. For neutral kaons, the situation is reversed. On the other hand, a u is twice as likely to produce a proton than a d [9] so that proton production is favored in pp interactions. The isospin effect is larger than the nuclear modifications on kaons and protons for  $p_T > 7.5 \text{ GeV}/c$ . The dominance of pion production by gluons and the assumption that u and d are equally likely to produce charged pions [9] leads to a negligible isospin effect for all  $p_T$ . Thus  $R_{AA}$  for pions is influenced only by the nuclear modifications. A similar conclusion was reached elsewhere [5].

Note that in both Figs. 2 and 3, the total  $R_{AA}$  closely follows the pion result. This is due to the relative fragmentation yields: the pion yield is significantly higher than the proton yield at all  $p_T$ , in contradiction with the data [1]. Reference [13] also showed that the  $p/\pi$ 

ratio was underpredicted by the fragmentation functions [9].

Other models may predict larger shadowing effects on  $R_A^i$ . For example, the shadowing model of Ref. [15], based on diffractive data from HERA, predicts large gluon shadowing for x < 0.01,  $R_A^g \approx 0.3$  at x = 0.001. They also predict significant antishadowing for x > 0.03, comparable to EKS98. The gluon shadowing grows rapidly when x < 0.01. This model should lead to significant reduction in  $R_{AA}$  for large rapidities at RHIC. However, in the region  $|y| \leq 1$ ,  $x \approx 0.02 - 0.1$ , nuclear effects are rather small and better constrained by data. Thus  $R_{AA}$  should not be significantly model dependent.

Models with strong gluon saturation and/or classical gluon fields, like the colored glass condensate [16], predict very different nuclear gluon densities. However,  $p_T > Q_s$ , the saturation scale predicted at RHIC [16]. In addition, at midrapidity, the relevant x values are not so small and are in a region where fixed-target data constrains the quark and antiquark modifications. Theoretical analysis indicates that the gluon distributions are also rather well constrained in the RHIC kinematic region [17]. These studies strongly limit the possible effect on  $R_{AA}$  near midrapidity.

At the LHC, where  $\sqrt{S_{NN}}=5.5$  TeV, the situation for lead on lead collisions will be very different. A hadron with  $p_T=5$  GeV/c (or a parton with  $p_T=10$  GeV/c) corresponds to  $x\approx 0.002$ , and shadowing is significant, reducing  $R_{AA}$  below 1. Away from y=0, even smaller x values are probed. Gluon dominance of minijet production extends to larger  $p_T$ , considerably reducing the effect of isospin. Thus nuclear modifications will be significant at the LHC.

In conclusion, nuclear shadowing cannot explain a significant fraction of the observed suppression of high- $p_T$  particles at RHIC. With the EKS98 parameterization and the nuclear isospin, at midrapidities  $1.0 < R_{AA} < 1.1$  for charged mesons and  $R_{AA} \approx 1$  for protons. Without the restriction  $|y| \leq 1$ , shadowing and isospin have a bigger effect on  $R_{AA}$ , with  $R_{AA} \approx 0.7$  at  $p_T = 2$  GeV/c, rising to 0.8 at  $p_T = 10$  GeV/c. Models with stronger nuclear effects may further reduce  $R_{AA}$  when all rapidities are considered. However, at midrapidity, no large effect on  $R_{AA}$  is expected from any model that reproduces the existing

lepton scattering data.

We thank K.J. Eskola for providing the shadowing routines. This work was supported in part by the Division of Nuclear Physics of the Office of High Energy and Nuclear Physics of the U. S. Department of Energy under Contract Number DE-AC03-76SF0098.

## REFERENCES

- K. Adcox et al. (PHENIX Collab.), arXiv:nucl-ex/0207009; Phys. Rev. Lett. 88, 022301 (2002); D. d'Enterria, in Proceedings of Quark Matter '02, Nantes, France, edited by H. H. Gutbrod et al., arXiv:hep-ex/0209051; J. Jia, in Proceedings of Quark Matter '02, Nantes, France, edited by H. H. Gutbrod et al., arXiv:nucl-ex/0209029.
- [2] C. Adler et al. (STAR Collab.), Phys. Rev. Lett. 89, 202301 (2002); J. L. Klay, in Proceedings of Quark Matter '02, Nantes, France, edited by H. H. Gutbrod et al., arXiv:nucl-ex/0210026.
- [3] C. Seife, Science **298**, 718 (2002); presented by J. Velkovska (PHENIX Collab.) at the Fall Meeting of the Division of Nuclear Physics of the American Physical Society, Oct. 9-12, 2002.
- [4] I. Vitev, M. Gyulassy and P. Lévai, Phys. Lett. B538, 282 (2002); arXiv:nucl-th/0204019.
- [5] S. Jeon, J. Jalilian-Marian and I. Sarcevic, arXiv:nucl-th/0208012.
- [6] J. J. Aubert et al. (European Muon Collab.), Nucl. Phys. B293 740, (1987); M. Arneodo, Phys. Rep. 240 301, (1994).
- [7] V. Emel'yanov, A. Khodinov, S. R. Klein and R. Vogt, Phys. Rev. C61, 044904 (2000).
- [8] R. D. Field, Applications Of Perturbative QCD (Addison-Wesley, Redwood City, CA, 1989).
- [9] B. A. Kniehl, G. Kramer and B. Pötter, Nucl. Phys. **B582**, 514 (2000).
- [10] A. D. Martin, R. G. Roberts, W. J. Stirling and R. S. Thorne, Eur. Phys. J. C4, 463 (1998); Phys. Lett. B443, 301 (1998).
- [11] K. J. Eskola, V. J. Kolhinen and P. V. Ruuskanen, Nucl. Phys. B535, 351 (1998); K.
   J. Eskola, V. J. Kolhinen and C. A. Salgado, Eur. Phys. J. C9, 61 (1999).

- [12] B. A. Kniehl, G. Kramer and B. Pötter, Nucl. Phys. **B597**, 337 (2001).
- [13] X. F. Zhang, G. Fai and P. Lévai, arXiv:hep-ph/0205008.
- [14] V. Emel'yanov, A. Khodinov, S. R. Klein and R. Vogt, Phys. Rev. Lett. 81, 1801 (1998);
   V. Emel'yanov, A. Khodinov, S. R. Klein and R. Vogt, Phys. Rev. C56, 2726 (1997).
- [15] L. Frankfurt, V. Guzey, M. McDermott and M. Strikman, JHEP 2, 27 (2002) [arXiv:hep-ph/0201230].
- [16] L. D. McLerran, Lect. Notes Phys. **583**, 291 (2002) [arXiv:hep-ph/0104285].
- [17] J. Jalilian-Marian and X. N. Wang, Phys. Rev. **D63**, 096001 (2001).

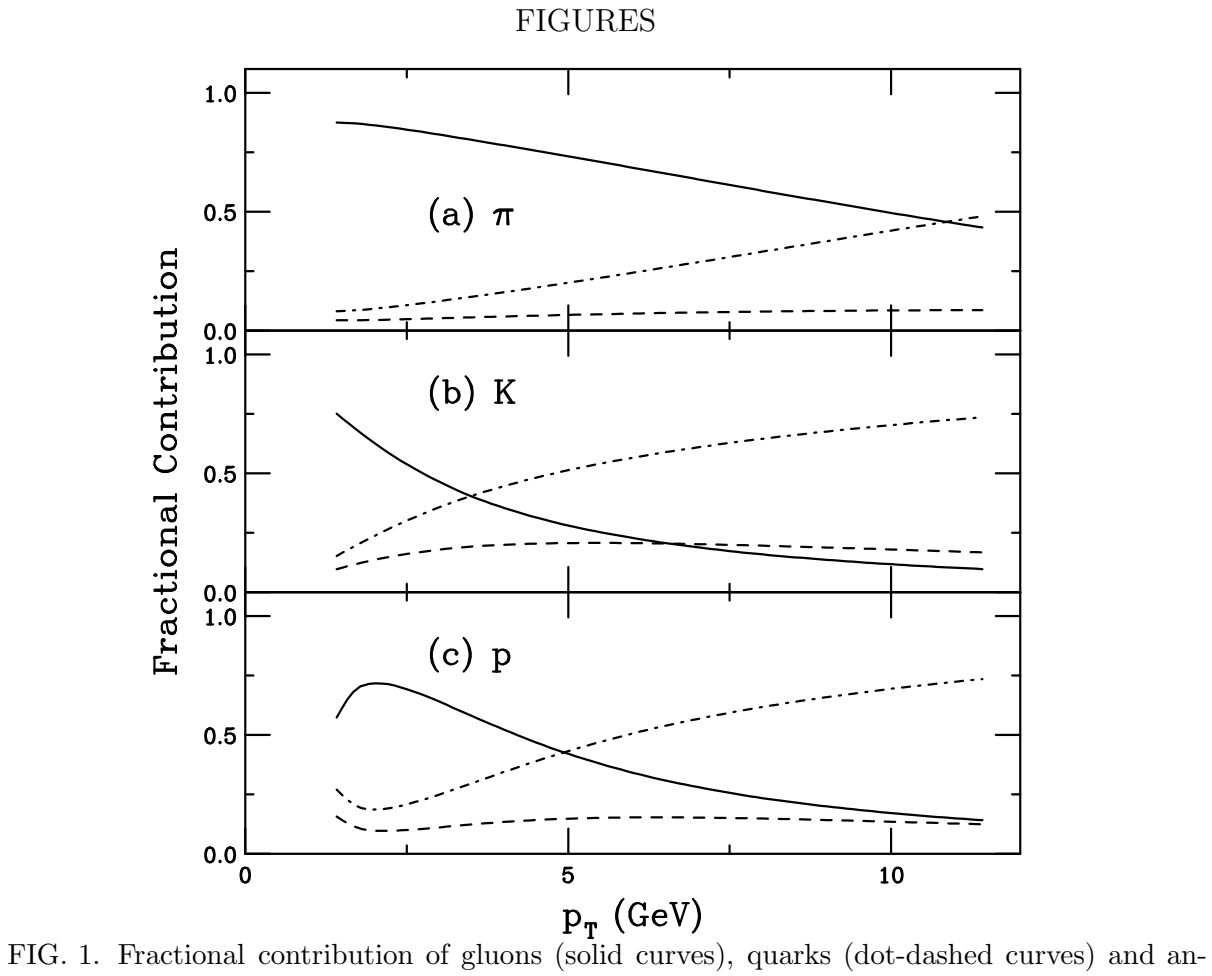
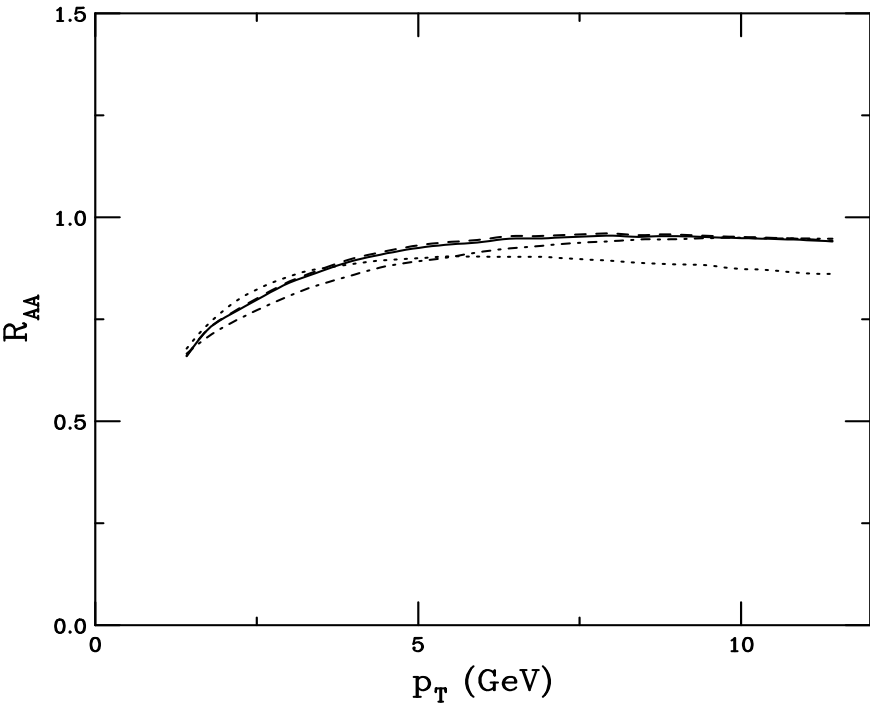


FIG. 1. Fractional contribution of gluons (solid curves), quarks (dot-dashed curves) and antiquarks (dashed curves) for (a) pion, (b) kaon, and (c) proton production in pp collisions at  $\sqrt{S} = 200$  GeV as a function of  $p_T$ .



 $\mathbf{p_T}$  (GeV)

FIG. 2.  $R_{AA}$  for pions (dashed curve), kaons (dot-dashed curve), protons (dotted curve) and the average over all hadrons (solid line) for gold-gold collisions at  $\sqrt{S_{NN}} = 200$  GeV as a function of  $p_T$ . Spatially averaged shadowing is used.

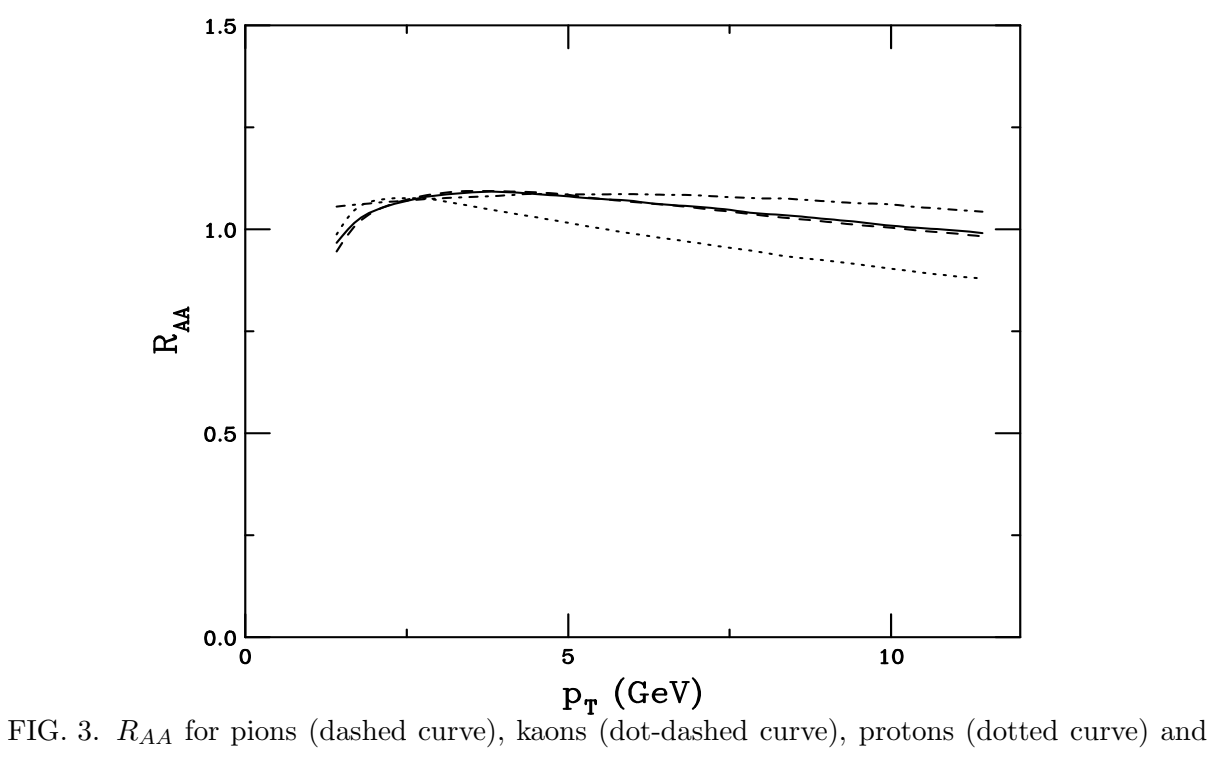


FIG. 3.  $R_{AA}$  for pions (dashed curve), kaons (dot-dashed curve), protons (dotted curve) and the average over all hadrons (solid line) for gold-gold collisions with  $|y| \le 1$  at  $\sqrt{S_{NN}} = 200$  GeV as a function of  $p_T$ . Spatially averaged shadowing is used.